

# Adaptive Multimodel Domain Decomposition in Fluid Mechanics

PATRICK LE TALLEC, FRANÇOIS MALLINGER \*

## 1 INTRODUCTION

Many practical problems of Fluid Mechanics require the simultaneous use of different physical models inside a given computational domain : local kinetic models must be used in shock or boundary layers when simulating rarefied flows, refined meshes are needed in recirculation regions or next to solid boundaries, wall laws are required when calculating turbulent flows around obstacles. For such problems, one must identify the domain where the local enriched model should be used, write adequate interface conditions for matching the local and the global models, and propose an adequate iterative algorithm for solving the resulting coupled problem without rewriting a full new computer code.

This paper presents a general domain decomposition strategy for tackling such situations, based on the following steps :

- approximate preliminary solution of the Navier-Stokes equations on the full computational domain;
- calculation of generalized residuals for detecting the regions where the present Navier-Stokes solution is inaccurate. For standard problems, these residuals are estimated by the approximate values of the second derivatives of basic physical quantities. For polyatomic rarefied flows, the residuals are obtained by plugging the Navier-Stokes solution into a generalized fourteen moments Grad equation specially developed for the occasion;
- adaptive construction and meshing of the different subdomains, finer models and finer grids being used in the regions of large residuals;
- development of adequate interface conditions. These interface conditions match inflow and outflow fluxes when coupling a local Boltzmann model with a global Navier-Stokes equation. They use mortar elements when matching convection dominated Navier-Stokes equations discretized on two nonoverlapping and nonmatching grids;
- solution of the coupled problem by a Dirichlet Neumann algorithm.

---

\*INRIA, Domaine de Voluceau, 78153 Le Chesnay Cedex, France. Email: patrick.letallec@inria.fr  
This work has been supported by the Hermes Research program

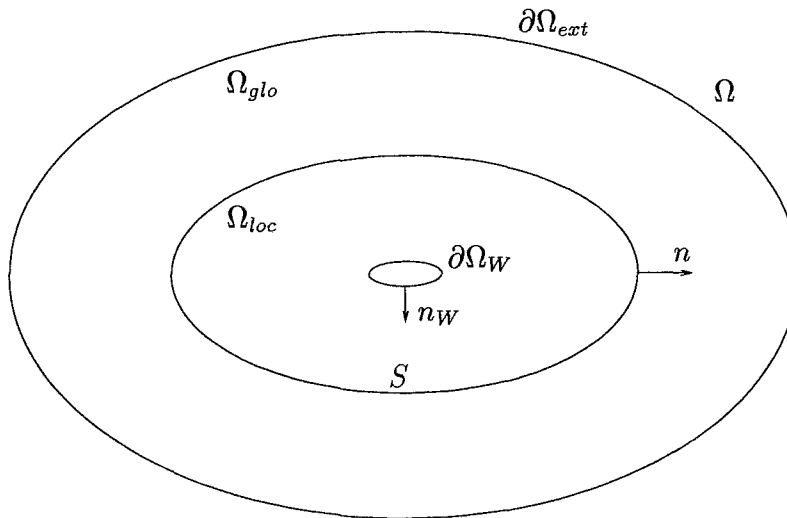


Figure 1: Decomposition of the domain in two subregions

This global strategy is presented below, with a particular emphasis on the simulation of rarefied gas flows.

## 2 THE PHYSICAL MODELS

### 2.1 Geometric description

We consider the flow of a gas in a global domain  $\Omega$  around a solid body of boundary  $\partial\Omega_W$  (Figure 1). We wish to split this domain into several nonoverlapping domains and to use the best available numerical model inside each subdomain. In general, one has at least to separate two different regions  $\Omega_{glo}$  and  $\Omega_{loc}$ . The domain  $\Omega_{loc}$  is a local domain which contains the obstacle, with internal boundary  $\partial\Omega_W$  and external boundary  $S$ . The domain  $\Omega_{glo}$  is a large domain, with an internal boundary  $S$  which surrounds the body and an external boundary  $\partial\Omega_{ext}$  which is the external boundary of the computational domain  $\Omega$ .

The subdomains  $\Omega_{glo}$  and  $\Omega_{loc}$  can be fixed arbitrarily at the beginning of the calculation or can be automatically adapted to the physical characteristics of the solution.

### 2.2 Basic Equations

On any subdomain  $\Omega_i$  where the flow can be reasonably described by these equations, the Navier-Stokes equations will be used with appropriate boundary conditions imposed on the body or on the different interfaces as specified later. These equations will be numerically solved by a SUPG solver written in entropic variables operating

on a given finite element triangulation of each local domain  $\Omega_i$  [8], [11]. The different finite element grids do not necessarily match at the subdomain interfaces.

Unfortunately, these equations cease to be valid at high altitudes corresponding to semi-rarefied regimes. At this level, slip effects can be observed in the boundary layer, shock begin to be thicker and the gas gets rarefied in the wake. Such local phenomena must then be described by kinetic models, such as the Boltzmann equation.

Let  $f$  be the density of gas particles at position  $x$  with velocity  $v$ , and internal energy  $I$ . The Boltzmann equation of rarefied gas dynamics characterizes this density as the solution of the integrodifferential equation ([4])

$$\frac{\partial f}{\partial t} + v \cdot \frac{\partial f}{\partial x} = Q(f, f).$$

The collision operator counts the particles which are gained or lost through intermolecular collisions. For molecular gas having internal degrees of freedom, it is defined by

$$Q(f, f) = \int_{\Delta} \left( \frac{f' f'_*}{(I' I'_*)^{\delta-1}} - \frac{f f_*}{(I I_*)^{\delta-1}} \right) B(I I_*^{\delta-1}) d\Delta,$$

$$d\Delta = dv_* dI_* [r(1-r)]^{\frac{\delta}{2}-1} dr R^2 (1-R^2)^{\delta-1} dR d\omega.$$

As usual we have used the notation

$$f = f(v, I), f' = f(v', I'), f_* = f(v_*, I_*), f'_* = f(v'_*, I'_*),$$

with  $(v, I)$  and  $(v_*, I_*)$  the velocities and internal energies of the colliding particles, and  $(v', v'_*)$  and  $(I', I'_*)$  the post collision velocities and internal energies. As in the monoatomic case, the collision direction  $\omega \in S^2$  is fixed and in a collision, we transform the vector  $(v, v_*, I, I_*)$  with  $v, v_* \in \mathbb{R}^3, I, I_* \geq 0$ , by setting

$$e^2 = \frac{1}{4} |v - v_*|^2 + I^2 + I_*^2 = \text{total energy of the collision},$$

$$g = v - v_* = \text{relative velocity},$$

and by defining the post collision velocities  $(v', v'_*)$  and energies  $(I', I'_*)$  by

$$v' + v'_* = v + v_*,$$

$$g' = v' - v'_* = 2Re\{g - 2\omega g \cdot \omega\} / |g|,$$

$$I'^2 = r(1-R^2)e^2, \quad I_*'^2 = (1-r)(1-R^2)e^2.$$

The factors  $R, r \in [0, 1]$  introduced in the collision operator determine the quantity of energy which is exchanged between internal and kinetic energy and between the two internal energies ([1], [3]). The term  $(II_*/I'I_*')^{\delta-1}$  is introduced to give the right value of

$$\gamma = \frac{\delta + 5}{\delta + 3},$$

in the limiting hydrodynamic equation of state  $p = (\gamma - 1)\rho e$ .

The collision cross section  $B$  measures the probability of collision of particles  $(v, I)$  and  $(v_*, I_*)$  with parameters  $(\omega, r, R)$ . In the general case, it is a function of all collision

invariants. In our simulations, we have used the classical Variable Hard Sphere model (VHS)

$$B = C|g|^{-2\alpha}|g \cdot \omega|R^{1-2\alpha},$$

which is the simplest model compatible with a Sutherland type viscosity law

$$\mu = KT^{\frac{1}{2}+\alpha},$$

at the Navier-Stokes limit. Here  $C$  and  $K$  are some constants.

This equation must be complemented by boundary conditions imposing the distribution of incoming particles. In the case of perfect accommodation on the body's surface, we would have

$$\begin{aligned} f(x, v, I, t) &= \rho_\infty M_{u_\infty, T_\infty}(v, I) \quad \text{if } v \cdot n < 0 \text{ at infinity,} \\ f(x, v, I, t) &= k M_{u_w, T_w}(v, I) \quad \text{if } v \cdot n_W < 0 \text{ on the body's surface,} \\ \int f(x, v, I, t) v \cdot n_W dv dI &= 0 \text{ on the body's surface,} \end{aligned}$$

with  $M_{u, T}$  denoting the Maxwellian distribution with mean velocity  $u$  and temperature  $T$

$$M_{u, T}(v, I) = \lambda_\delta \frac{\rho I^{\delta-1}}{T^{(3+\delta)/2}} \exp\left(-\frac{|v-u|^2 + 2I^2}{2T}\right).$$

More elaborate boundary conditions can also be introduced ([4]).

### 2.3 Transition between Boltzmann and Navier-Stokes

When the gas is dense, solving Boltzmann equation is very expensive or out of reach. Therefore, we wish to solve Boltzmann equations on very small subdomains, and to be able to realise smooth transitions or couplings between these Boltzmann solutions and cheaper Navier-Stokes solutions. For this purpose, the best way is to introduce an asymptotic kinetic model, approximating the Boltzmann equation, and degenerating to the Navier-Stokes model when the gas gets dense.

For monoatomic gases, this is classically achieved by introducing the so-called Chapman-Enskog or Grad expansions [6]. For more realistic polyatomic gas having internal energies, we first need to extend these approaches.

To obtain such a polyatomic generalisation of Grad's thirteen moments expansion, we first assume that  $f$  can be represented as a linear combination of Hermite polynomials, given here for a diatomic gas ( $\delta = 2$ ), by

$$\begin{aligned} f &= f^{(0)} \left[ 1 + \frac{p_{ij}}{2pR_gT} ((v-u)_i(v-u)_j - I^2 \delta_{ij}) \right. \\ &\quad \left. + \frac{1}{14} \frac{S_i (v-u)_i}{pR_gT} \left( \frac{|v-u|^2}{R_gT} + \frac{2I^2}{R_gT} - 7 \right) \right], \\ f^{(0)} &= \frac{\sqrt{2}\rho I^{\delta-1}}{(2\pi)^{\frac{3}{2}}(R_gT)^{(3+\delta)/2}} \exp\left(-\left(\frac{|v-u|^2 + 2I^2}{2R_gT}\right)\right). \end{aligned}$$

This ansatz can be either postulated or derived as the trace of the Grad's expansion of a monoatomic gas in dimension  $(3 + \delta)$  ([7]). From the orthogonality of the Hermite polynomials, the thermodynamic coefficients  $\rho$  (density),  $p$  (pressure),  $p_{ij}$  (the opposite of the viscous stress tensor),  $S_i = 2q_i$  (two times the heat conduction vector) correspond to the usual definition

$$\begin{aligned}\rho &= \int f \, dv dI, \\ \rho u_i &= \int v_i f \, dv dI, \\ p &= \rho R_g T = \frac{1}{\delta + 3} \int \left( \frac{|v - u|^2}{2} + I^2 \right) f \, dv dI, \\ \sigma_{ij} &= - \int (v - u)_i (v - u)_j f \, dv dI, \\ q_i &= \int (v - u)_i \left( \frac{|v - u|^2}{2} + I^2 \right) f \, dv dI \\ p_{ij} &= -\sigma_{ij} - p \delta_{ij}, \\ S_i &= 2q_i.\end{aligned}$$

To identify these unknown thermodynamic moments, we now report the above expression of  $f$  into the Boltzmann equation and integrate the resulting equation against the 14 moments

$$K_{14} = \begin{pmatrix} 1 \\ v_i \\ v_i v_j \\ 2I^2 \\ v_i(|v|^2 + 2I^2) \end{pmatrix}.$$

This yields the final reduced variational kinetic system

$$\frac{\partial}{\partial t} \int K_{14} f \, dI dv + \frac{\partial}{\partial x_k} \int K_{14} v_k f \, dI dv = \int K_{14} Q(f) \, dI dv. \quad (1)$$

If we calculate the different integrals in (1) and take into account the particular expression of  $f$ , after lengthy algebraic calculations, we can rewrite this variational equation as the following Grad system of partial differential equations [7]

- Navier-Stokes Conservation laws

$$\begin{aligned}\frac{\partial \rho}{\partial t} + u_k \cdot \frac{\partial \rho}{\partial x_k} + \rho \frac{\partial u_k}{\partial x_k} &= 0, \\ \frac{\partial u_i}{\partial t} + u_k \cdot \frac{\partial u_i}{\partial x_k} - \frac{1}{\rho} \frac{\partial \sigma_{ik}}{\partial x_k} &= 0, \\ \frac{\partial p}{\partial t} + \frac{2}{5} p_{ik} \frac{\partial u_i}{\partial x_k} + u_k \frac{\partial p}{\partial x_k} + \frac{7}{5} p \frac{\partial u_k}{\partial x_k} + \frac{1}{5} \frac{\partial S_k}{\partial x_k} &= 0,\end{aligned}$$

- differential generalisation of Navier-Stokes constitutive laws

$$\begin{aligned}
& \frac{\partial p_{ij}}{\partial t} + \frac{\partial u_k p_{ij}}{\partial x_k} + \frac{1}{7} \left( \frac{\partial S_i}{\partial x_j} + \frac{\partial S_j}{\partial x_i} - \frac{2}{5} \frac{\partial S_k}{\partial x_k} \delta_{ij} \right) \\
& + p_{jk} \frac{\partial u_i}{\partial x_k} + p_{ik} \frac{\partial u_j}{\partial x_k} - \frac{2}{5} p_{kl} \frac{\partial u_l}{\partial x_k} \delta_{ij} \\
& + p \left( \frac{\partial u_i}{\partial x_j} + \frac{\partial u_j}{\partial x_i} - \frac{2}{5} \frac{\partial u_k}{\partial x_k} \delta_{ij} \right) = J_{ij}^{(2)}, \\
& \frac{\partial S_i}{\partial t} + \frac{\partial u_k S_i}{\partial x_k} + \frac{9}{7} S_k \frac{\partial u_i}{\partial x_k} + \frac{2}{7} S_i \frac{\partial u_k}{\partial x_k} + \frac{2}{7} S_k \frac{\partial u_k}{\partial x_i} \\
& + \frac{2}{\rho} p_{il} \frac{\partial \sigma_{lk}}{\partial x_i} + 2 R_g T p_{il} \frac{\partial p_{ik}}{\partial x_k} + 9 p_{ik} \frac{\partial R_g T}{\partial x_k} \\
& + 7 p \frac{\partial R_g T}{\partial x_i} = J_i^{(3)} - 2 u_l J_{il}^{(2)}.
\end{aligned}$$

Right Hand Sides  $J_{ij}^{(n)}$  are explicit integrals of collision cross-sections and can be expressed as functions of the different thermodynamic variables ([9]).

To derive the Navier-Stokes equation, we then suppose in addition that the fluid is close to equilibrium so that moments  $p_{ij}$  or  $S_i$  and gradients of thermodynamic variables remain small. At first order, the differential constitutive laws then reduce to the standard laws

$$\begin{aligned}
p_{ij} &= -\mu \left( \frac{\partial u_i}{\partial x_j} + \frac{\partial u_j}{\partial x_i} \right) - \lambda \frac{\partial u_k}{\partial x_k} \delta_{ij}, \\
S_i &= -2\kappa \frac{\partial T}{\partial x_i},
\end{aligned}$$

with transport coefficients

$$\begin{aligned}
\mu &= \frac{30 (R_g T)^{1/2}}{C \pi^{1/2}}, \\
\kappa &= \frac{1323}{570} R_g \mu, \\
\lambda &= - \left( \frac{2}{5} + \frac{4}{375} \right) \mu.
\end{aligned}$$

With this simplification, we get the Navier-Stokes equations as the limiting case of a Grad's fourteen moments expansion. As a byproduct, which will be the key for closing our hierarchy of models and constructing our coupling strategy, we also obtain the polyatomic kinetic distribution associated to the Navier-Stokes solution as

$$\begin{aligned}
f_{NS} &= f^{(0)} \left[ 1 - \frac{2\mu}{p R_g T} \left( (v_i - u_i)(v_j - u_j) - \left( \frac{2}{5} + \frac{4}{375} \right) |v - u|^2 \delta_{ij} \right. \right. \\
& + \left. \left( 1 - \left( \frac{3}{5} + \frac{2}{375} \right) \right) I^2 \delta_{ij} \right) \frac{\partial u_i}{\partial x_j} \\
& \left. - \frac{\kappa}{7} \frac{(v - u)_i}{p R_g T} \left( \frac{|v - u|^2}{R_g T} + \frac{2I^2}{R_g T} - 7 \right) \frac{\partial T}{\partial x_i} \right].
\end{aligned}$$

This distribution generalises the classical monoatomic distribution originally introduced by Chapman-Enskog and Grad.

**Remark 1** *The Grad's equation introduced above as an intermediate step between Boltzmann and Navier-Stokes is not a good model by itself. Its physical relevance is not guaranteed, and mathematically it loses the positivity and hyperbolicity properties of the underlying Boltzmann equation. What is expected nevertheless, and what is verified in our numerical test, is that the difference between Grad and Navier-Stokes is a good measure of the amount of disequilibrium in the fluid, and therefore of the local lack of validity of our Navier-Stokes solution.*

### 3 ADAPTIVE CONSTRUCTION OF THE SUB-DOMAINS

Our basic problem is now to find the legitimate Navier-Stokes domain, or equivalently to find the Boltzmann zone  $\Omega_{loc}$  where the Navier-Stokes solution  $f_{NS}$  is not an adequate solution of our problem, and where we should therefore solve the kinetic Boltzmann equation. For this purpose, we use our above model hierarchy and simply observe the quality of the Navier-Stokes distribution as solution of the finer Boltzmann equation. This original distribution is obtained by solving the Navier Stokes equations on the whole domain with say wall laws or slip boundary conditions at the wall. Plugging this solution into Boltzmann equation leads to the following variational residual

$$\begin{aligned} & \int \varphi(v, I) \left[ \frac{\partial f_{NS}}{\partial t} + v \cdot \frac{\partial f_{NS}}{\partial x} - Q(f_{NS}, f_{NS}) \right] dv dI \\ &= \int \varphi(v, I) R(f_{NS}) dv dI = R_\varphi(f_{NS})(x, t), \quad \forall \varphi, \forall x \in \Omega. \end{aligned}$$

As such, this residual is still too complex to compute. Therefore, we restrict ourselves to the test functions  $\varphi$  used in Grad's 14 moments derivation. With this choice, we can compute one local residual per finite element function  $\psi_N$  given by

$$\begin{aligned} R_N = & \frac{1}{\text{VolCell}_N} \left\| \int_{\Omega} -u_k p_{ij} \frac{\partial \psi_N}{\partial x_k} \right. \\ & - \frac{1}{7} \left( S_i \frac{\partial \psi_N}{\partial x_j} + S_j \frac{\partial \psi_N}{\partial x_i} - \frac{2}{5} S_k \frac{\partial \psi_N}{\partial x_k} \delta_{ij} \right) \\ & + \left( p_{jk} \frac{\partial u_i}{\partial x_k} + p_{ik} \frac{\partial u_j}{\partial x_k} - \frac{2}{5} p_{kl} \frac{\partial u_l}{\partial x_k} \delta_{ij} \right. \\ & \left. \left. + p \left( \frac{\partial u_i}{\partial x_j} + \frac{\partial u_j}{\partial x_i} - \frac{2}{5} \frac{\partial u_k}{\partial x_k} \delta_{ij} \right) - J_{ij}^{(2)} \right) \psi_N \right\|. \end{aligned}$$

This residual is simply the norm of the residual of Grad's equation in the  $p_{ij}$  moment, when used with the available Navier-Stokes solution. From our previous remark, this difference should be a good indicator of disequilibrium in the fluid, and therefore of the local relevance of the Navier-Stokes equations.

We now choose the Boltzmann region  $\Omega_{loc}$  as the region of  $\Omega$  where this residual is the largest.

In practice, recovering the original domain by an unstructured adapted Navier-Stokes grid and a cartesian Boltzmann grid, we identify this region by the following sequence of operations :

1. calculation of a global, numerically accurate Navier-Stokes solution;
2. calculation of the above residual on each Navier-Stokes node;
3. interpolation and smoothing of this residual on the cartesian grid;
4. definition of the Boltzmann domain  $\Omega_{loc}$  as the set of cartesian cells where the residual is above a user defined threshold;
5. calculation of the internal Navier-Stokes interface by spline interpolation of the jagged Boltzmann interface;
6. automatic meshing of the external Navier-Stokes zone by a Voronoi algorithm, the size of the elements being equidistributed with respect to the Hessian of characteristic flow variables.

We illustrate below this strategy on the following example

$$\begin{aligned}
 \gamma &= \frac{7}{5}, Pr = \frac{18}{25} \\
 \text{Angle of attack} &= 30 \text{ degrees} \\
 M_\infty &= 20 \\
 Reynolds &= 5000/m, 50000/m \\
 T_\infty &= \frac{1}{\gamma R_g M_\infty^2} \\
 u_\infty &= 1 \\
 \rho_\infty &= 1 \\
 T_W &= 6 T_\infty \\
 u_W &= 0
 \end{aligned}$$

The Navier-Stokes solution is calculated by a SUPG code provided by Dassault, using a mesh of 6882 nodes. We present below the original Navier-Stokes mesh, the calculated residual isolines defining Boltzmann and Navier-Stokes regions, that we compare to the amount of rarefied disequilibrium predicted by a global Boltzmann calculation. We observe that apart from boundary problems induced by the noslip boundary condition in the Navier-Stokes solution, both the Grad's residual and the global kinetic solution predict the same geometry for the rarefied domain (figures 2, 3, 4, 5). Similar results can be found for denser flows in ([9]).

## 4 THE COUPLED PROBLEM

Once knowing the adaptive partition of our original domain between a Navier-Stokes and a Boltzmann domain, we need to formulate and solve the resulting coupled problem. For this purpose, we will first introduce the coupling strategy in the



general hyperbolic case of a Boltzmann-Boltzmann coupling and then degenerate one Boltzmann domain to the limiting Navier-Stokes model.

Let us for the moment consider the domain as splitted into two nonoverlapping subdomains  $\Omega_1$  and  $\Omega_2$  with external unit normal vector  $n_1$  and  $n_2$ , and interface  $\Gamma$ . By restricting Boltzmann equation to each subdomain and decomposing the interface continuity condition  $(f_1 - f_2)v \cdot n_i = 0$  along incoming subdomain characteristics, we can decompose the original Boltzmann equation into the coupled set of well-posed subproblems

$$\begin{aligned} \operatorname{div}_x(vf_1) &= Q(f_1, f_1) \text{ in } \Omega_1 \times \mathbb{R}^3, \\ f_1(x, v, I) &= f_2(x, v, I) \text{ on } \Gamma \text{ if } v \cdot n_1 < 0, \end{aligned}$$

$$\begin{aligned} \operatorname{div}_x(vf_2) &= Q(f_2, f_2) \text{ in } \Omega_2 \times \mathbb{R}^3, \\ f_2(x, v, I) &= f_1(x, v, I) \text{ on } \Gamma \text{ if } v \cdot n_2 < 0. \end{aligned}$$

This coupled problem can then be solved by the fixed point Dirichlet-Neumann type iterative procedure [10]

- guess  $f_2(x, v, I)$  on incoming characteristics  $v \cdot n_1 < 0$ ,
- solve the resulting subproblem on  $\Omega_1$ ,
- with the resulting value  $f_1(x, v, I)$  imposed on the incoming characteristics  $v \cdot n_2 < 0$ , solve the subproblem on  $\Omega_2$ ,
- use the result to update  $f_2(x, v, I)$  on the interface and reiterate.

This numerical strategy seems to be quite efficient, although a few theoretical results are yet unsolved : well-posedness of each subproblem (this can be proved for a BGK kinetic problem, not for Boltzmann), cost and noise control of each local numerical Boltzmann solution when using Monte-Carlo techniques, convergence of the fixed point iterations. For the time being, such convergence is only proved in the absence of collision terms [5].

Despite these theoretical weaknesses, we can easily extend the above strategy to the Navier-Stokes Boltzmann coupling, simply by replacing  $f_1$  on  $\Omega_1$  by its Navier-Stokes approximation

$$f \approx f_{NS}.$$

The interface boudary condition is then transformed into

$$\begin{aligned} f_2(v, I) &= f_{NS}(v, I) \text{ on } \Gamma \text{ if } v \cdot n_2 < 0, \\ f_{NS}(v, I) &= f_2(v, I) \text{ on } \Gamma \text{ if } v \cdot n_1 < 0. \end{aligned}$$

The first condition is imposed as boundary condition in the Boltzmann domain. The second condition is imposed as a boundary condition in the Navier-Stokes region by taking its velocity average

$$Flux(U, n) = Flux_+(U, n) + Flux_-(U, n), \quad (2)$$

$$Flux_+(U, n) = \int_{v \cdot n > 0} \begin{bmatrix} 1 \\ v \\ v^2/2 + I^2 \end{bmatrix} v \cdot n f_{NS}(x, v, I) dv dI,$$

$$Flux_-(U, n) = \int_{v \cdot n < 0} \begin{bmatrix} 1 \\ v \\ v^2/2 + I^2 \end{bmatrix} v \cdot n f_2(x, v, I) dv dI.$$

With this new boundary condition, our Dirichlet-Neumann loop reduces to the following sequence of operations already described in [2]

1. Solve few steps of the local Boltzmann problem

$$\begin{aligned} \frac{f^n - f^{n-1}}{\Delta t} + \operatorname{div}_x(v f^n) &= Q(f^n, f^n)(x, v, I) \text{ on } \Omega_2, \\ f^n(x, v, I) &= f_{NS}(x, v, I) \text{ on } \Gamma \text{ if } v \cdot n_2 < 0, \\ f^n(x, v, I) &= \text{Maxwellian on body.} \end{aligned}$$

2. From  $f^n$ , compute the half fluxes  $Flux_-$  entering the internal boundary of Navier-Stokes region
3. With these imposed fluxes  $Flux_-$ , using the mixed boundary condition (2) on the interface and usual boundary conditions at infinity, integrate the Navier-Stokes equations a few steps in time on the external domain and go back to the Boltzmann problem.

In all our numerical tests, we have used 5 such global iterations.

We have first tested this algorithm by computing the two-dimensional flow around an ellipse with the physical data

$$\begin{aligned} \gamma &= \frac{5}{3}, Pr = \frac{1}{3} \\ \text{Angle of attack} &= 30 \text{ degrees} \\ M_\infty &= 20 \\ Reynolds &= 5000/m \\ T_\infty &= 167.3K \\ u_\infty &= 5672m/s \\ \rho_\infty &= 1 \\ T_W &= 5.6T_\infty \\ u_W &= 0 \end{aligned}$$

The corresponding results are then validated by comparing them to the solution of a global Boltzmann simulation (figures 6, 7 and 8). We observe that the coupled solution is quite smooth at the interface and coincides with the global Boltzmann solution, including at the wall, and this is achieved at a smaller computational cost.

## 5 CONCLUSION

The proposed multimodel coupling numerical strategy appears to be operational for polyatomic gases while using adaptive domain splitting. For industrial flexibility, it was implemented by chaining independent Navier-Stokes and Boltzmann codes within an unique shell script.

The work to be done concerns the cost and noise control in the numerical solution of the local Boltzmann problem, the improvement of the rarefied model hierarchy by deriving more consistent asymptotic expansions (Levermore) preserving positivity and hyperbolicity of the asymptotic limit, and the generalisation to the numerical treatment of turbulent boundary layers via asymptotic wall laws.

## References

- [1] J.F. Bourgat, L. Desvillettes, P. Le Tallec, B. Perthame, "Microreversible collisions for polyatomic gases and Boltzmann's theorem" ,*J. Mech., B/Fluids*, 13, 1994.
- [2] J.F. Bourgat, P. Le Tallec, F. Mallinger, B. Perthame, Y.Qiu, "Couplage Boltzmann Navier-Stokes", *Rapport de Recherche Inria N 2281*, Mai 1994.
- [3] C. Borgnakke, P.S. Larsen, Statistical collision model for Monte-Carlo simulation of polyatomic gas mixtures. *J. C.P.* 18, 405-420 (1975).
- [4] C. Cercignani, The Boltzmann equation and its applications. Springer-Verlag, 1975.
- [5] F. Gastaldi, L. Gastaldi, "On a domain decomposition approach for the transport equation: theory and finite element approximations", *IMA Journal of Numerical Analysis*, Vol. 14, 1993.
- [6] H. Grad, On the Kinetic Theory of Rarefied Gases. *Comm. Pure and Appl. Math.*, 49, 331-407, 1949.
- [7] P. Le Tallec, F. Mallinger, "Modélisation d'un gaz Polyatomique, Equations de Grad Généralisées et Validité de la Solution des Equations de Navier-Stokes" *Rapport de contrat final - Hermes* , April 1995.
- [8] M. Mallet, "A finite element method for computational fluid dynamics", *Ph.D. Thesis*, Stanford University, 1985 .
- [9] F. Mallinger, "Couplage adaptatif des équations de Boltzmann et de Navier-Stokes", *Thèse d'Université*, Paris Dauphine, à paraître 1995.
- [10] L.D. Marini, A. Quarteroni, " A relaxation procedure for Domain Decomposition Methods using Finite Elements", *Num. Math.*, 55, 575-598, 1989.
- [11] F. Shakib, "Finite element analysis of the compressible Euler and Navier-Stokes equations", *Ph.D. Thesis*, Stanford University, 1988 .

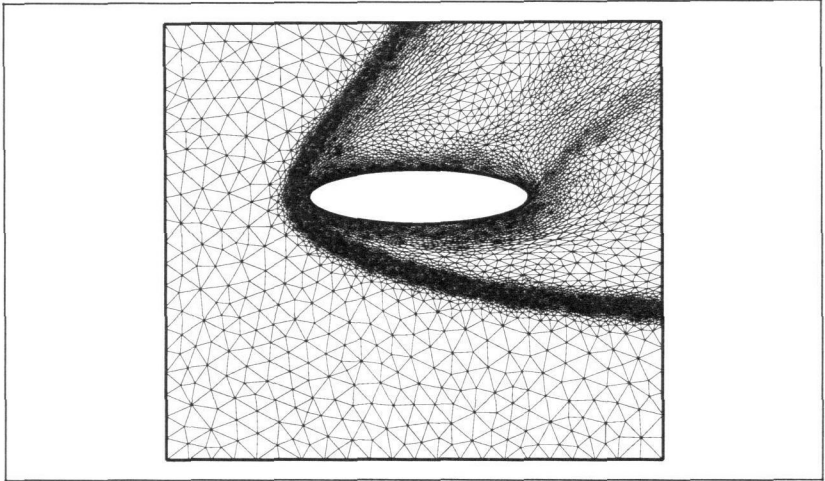


Figure 2: Navier-Stokes mesh: 6882 nodes. The Navier-Stokes solution is computed with no-slip boundary condition on the wall.

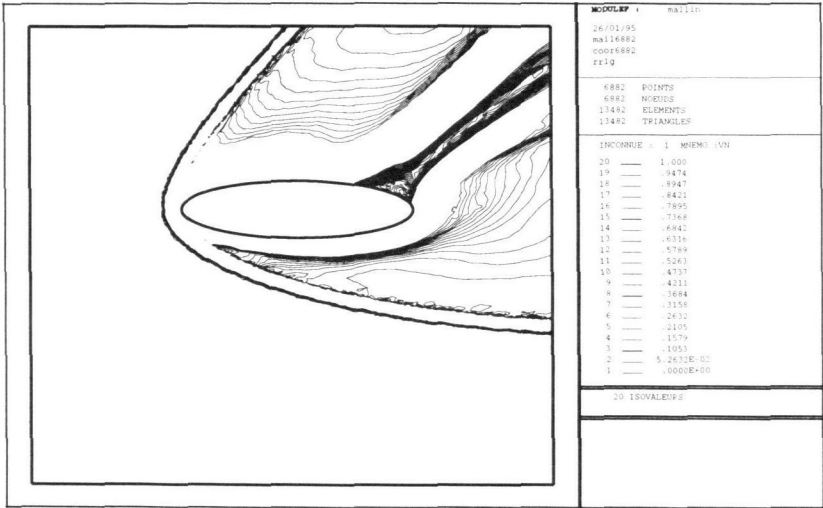


Figure 3: Grad criterion:  $Re=5000/m$ . We draw only the isolines between 0 and 1. The white zone defines the Boltzmann domain.

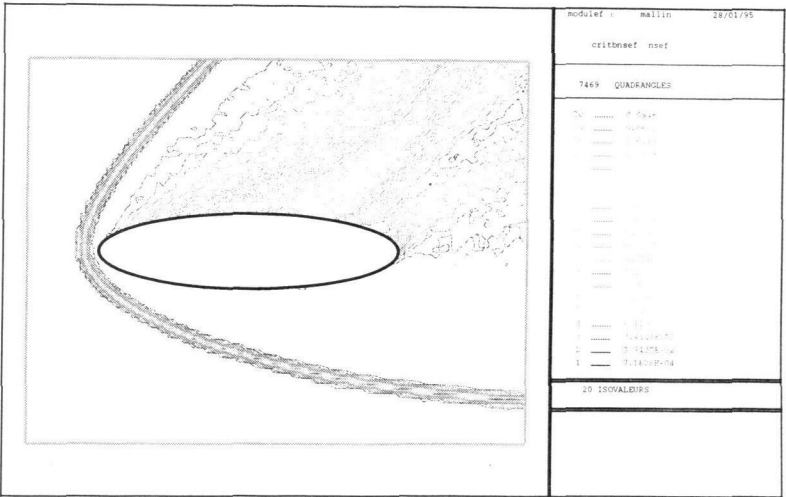


Figure 4: Boltzmann criterion estimated by a kinetic simulation. We verify that the Boltzmann region here is quite similar, except under the body. This difference is due to the bad boundary condition use in the Navier-Stokes computation.

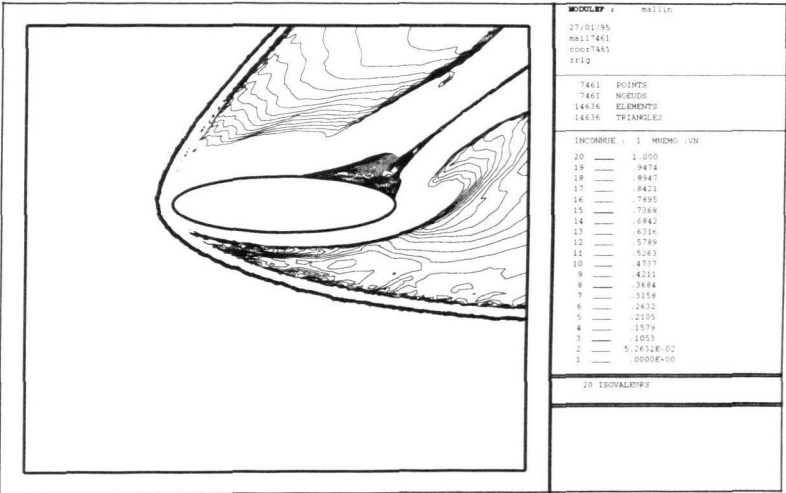


Figure 5: Grad criterion: Re=50000/m.

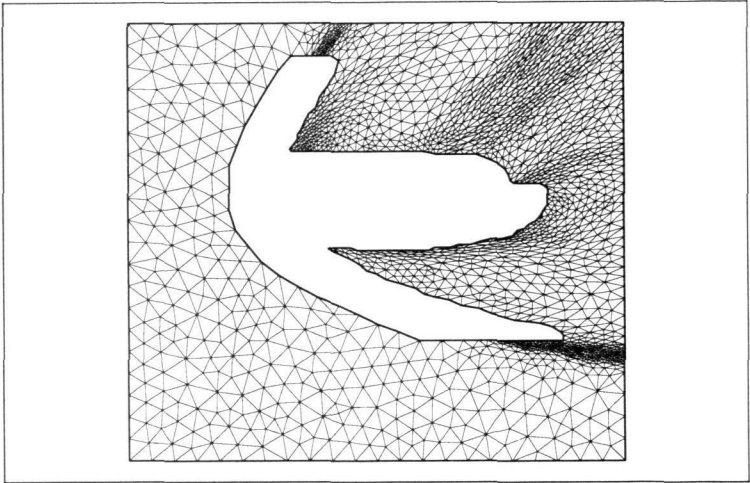


Figure 6: Navier-Stokes mesh to compute a coupled solution. The internal boundary is obtained thanks to the criterion. The mesh is adapted with the global initial Navier-Stokes solution.

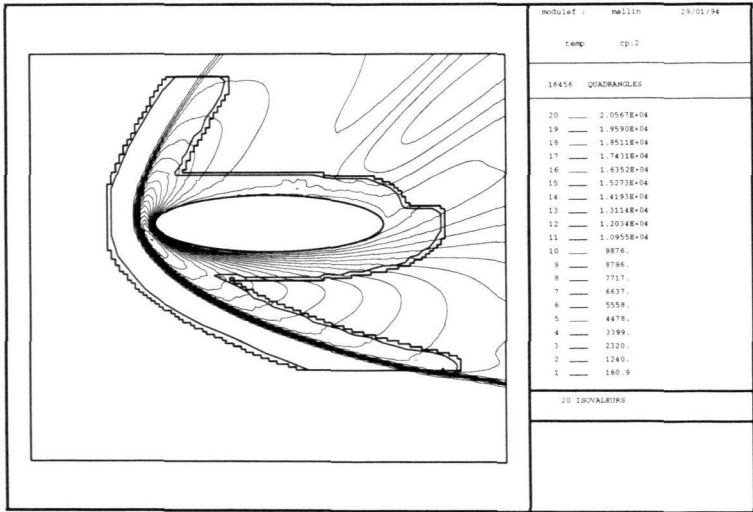


Figure 7: Temperature isolines of the coupled solution. The continuity of the isolines at the coupling interface is very good.

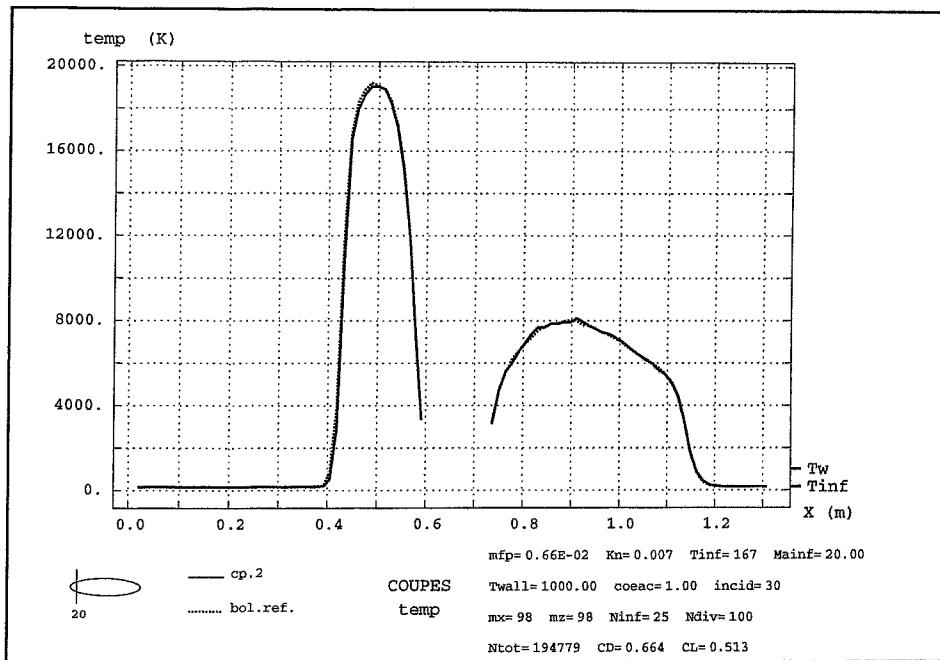


Figure 8: Cross section of the temperature. Superposition of the Boltzmann solution (dotted line) and the coupled solution (continuous line). The coupled solution is very good compared to the Boltzmann reference solution and recovers the right temperature jumps at the wall.